

Model independent phase equilibrium constraints on the ferrosilite activity in the binary Fe-Mg orthopyroxene solid solution

LEONID Y. ARANOVICH*

Institute of Experimental Mineralogy RAS, Chernogolovka, 142432 Russia

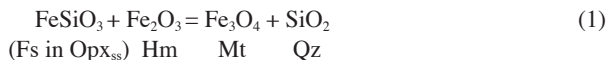
ABSTRACT

Compositional reversals of orthopyroxene solid solution (Opx) on the enstatite (En, MgSiO₃)-ferrosilite (Fs, FeSiO₃) join equilibrated with hematite (Hm, Fe₂O₃), magnetite (Mt, Fe₃O₄), and quartz (Qz) were obtained in piston-cylinder apparatus in the pressure range 10–25 kbar at temperatures of 800 and 950 °C. A double-capsule technique with the Hm-Mt external buffer was employed to ensure the presence of both Fe oxides in the run products. Starting materials were crystalline mixtures of synthetic Opx with $X_{\text{Fs}} [= \text{Fe}/(\text{Fe}+\text{Mg})] = 0.05$ and 0.45, reagent Mt, Hm, and natural Qz. Run products were carefully examined using optical microscopy, back-scattered (BSE) imaging, and wavelength dispersive electron microprobe analysis. Despite the differences in the rates of forward and backward reactions $\text{Fs (in Opx)} + \text{Hm} = \text{Mt} + \text{Qz}$ (1), very tight compositional brackets (less than 0.01 X_{Fs}) were obtained at each P - T . At 800 °C, midpoints of the compositional brackets are: 0.195/10 kbar, 0.24/15, 0.29/20, and 0.34/25; at 950 °C: 0.21/15 kbar, 0.25/20, and 0.295/25 kbar. Activities of Fs, recalculated from these compositions using either Berman and Aranovich (1996) or Holland and Powell (1998) data sets for the pure end-member reaction (1), show negative deviation from ideal mixing. Strongly temperature dependent enthalpy of mixing is required to make these activity values consistent with the configurational entropy of the solid solution deduced from the site occupancy measurements. A simple mixing model with a linearly varying temperature-dependent W term, similar to that of Berman and Aranovich (1996), adequately reproduces the experimental data.

INTRODUCTION

Activity-composition relations in the binary Fe-Mg orthopyroxene (Opx) are important for a number of quantitative geochemical applications, including geothermobarometry (e.g., Berman and Aranovich 1996), upper mantle geooxymetry (e.g., Wood and Virgo 1989), and melt modeling (Ghiorso and Sack 1995). This system also bears theoretical interest as a possible example of a microscopically ordered solid solution that yet exhibits macroscopically positive deviation from ideality (e.g., Sack and Ghiorso 1989; Yang and Ghose 1994; Holland and Powell 1996). This possibility for Opx was, however, challenged by several authors (Sack 1980; Aranovich and Kosyakova 1987; Berman and Aranovich 1996) who obtained negative excess Gibbs free energy values in a wide temperature range up to about 1000 °C. The conflicting results have been obtained regardless of whether the site occupancy data were (cf., Sack 1980; Aranovich and Kosyakova 1987; vs. Sack and Ghiorso 1989) or were not (cf., Berman and Aranovich 1996; vs. von Seckendorff and O'Neill 1993) included in the processing. It appears, therefore, that the discrepancy among the various modeling results is mostly due to the ambiguities in the experimental data involved rather than to the differences in the models employed in the modeling. The major ambiguity may be readily attributed to the presence in most experimental phase-equilibrium studies involving the Opx solid solution (Aranovich and Kosyakova 1987; Bohlen et al. 1980; Lee and Ganguly 1988; Fonarev and Konilov 1986; von

Seckendorff and O'Neill 1993) of one or more other phases of variable composition, which has led to the largely uncertain and correlated model parameters (e.g., von Seckendorff and O'Neill, 1993; Berman and Aranovich, 1996). This ambiguity is also true for the activity calculations based on the site occupancy measurements, where both M1 and M2 sites have been treated as non-ideal solutions (e.g., Yang and Ghose 1994). To avoid this ambiguity in constraining the Fe-Mg Opx mixing properties, this report presents reversed experimental data on the reaction:



The advantage of employing this reaction, from both experimental and modeling standpoints, is that it involves only one solid solution phase (Opx) whose equilibrium composition can be approached from opposite directions at fixed P - T conditions.

EXPERIMENTAL METHODS

Experiments on Reaction 1 were carried out in a 1.91 cm (3/4 inch) diameter piston-cylinder apparatus with NaCl as a pressure medium and a graphite heater sleeve. Sample geometry was identical to that of Aranovich and Newton (1999). Pressures are believed accurate to ± 300 bars. Temperature was measured with W-3% Re vs. W-25% Re thermocouples that were in virtual contact with the noble metal sample capsules during the experiments. Run temperatures are believed to be accurate to ± 5 °C. In order to stabilize both Fe oxides, all experiments of the present study were carried out at relatively high oxygen fugacity values corresponding to the hematite-magnetite (HM) buffer. An initial buffer charge of about 40 mg of hematite and 4 mg of H₂O was sealed by arc-welding into a segment of 5 mm gold tubing along with the 3 mm sealed platinum sample capsule. The hematite in the outer Au capsule was typically about 50–70% converted to magnetite during an

*E-mail: lyaranov@iem.ac.ru

experiment. The sample capsules contained 5–6 mg of crystalline starting materials and about 1 mg of doubly distilled H₂O. Platinum is known to dissolve appreciable amounts of Fe in high-temperature experiments. Iron loss to the capsule walls was not, however, a serious consideration of this study because of the relatively low temperature of the runs, high oxygen fugacity, and, most importantly, oversaturation of the studied system in respect to Fe. Indirect evidence of the insignificant Fe solubility in Pt under the run conditions of this study comes from very small weight gain observed for the Pt capsules after the runs despite the fact that during the runs they were almost completely immersed in the hematite-magnetite mix.

Starting materials for the reversal runs on Reaction 1 were finely ground and homogenized powdered mixtures of minerals of the reaction taken in stoichiometric proportion. Commercially available reagent grade hematite and magnetite were used along with natural quartz from Lisbon, Maryland. Two starting Opx compositions with X_{Fs} [=Fe/(Fe + Mg)] = 0.05 and 0.45 (Table 1) were synthesized from mechanical mixes of reagent grade MgO, Fe-oxalate, and silica in sealed gold capsules, with about 10 wt% H₂O and 5 wt% excess (relative to the stoichiometric amount) silica to saturate the fluid phase. Synthesis conditions are given in Table 1. The synthesis products were Opx crystals with very subordinate amounts of quartz. Optical, X-ray diffraction (XRD), and BSE imaging analysis revealed no other phases. The product Opx formed mostly prismatic grains with a fairly even grain size distribution ranging from 4–5 by 10–15 μm for the Fe-rich compositions to about 2–3 by 7–10 μm for the Mg-rich one (Figs. 1a, 1b). Microprobe analysis of the synthetic starting orthopyroxenes proved them chemically homogeneous within the analytical uncertainties of the method ($\pm 2\%$ of the amount of oxides present), and practically identical to the expected theoretical composition (Table 1). Unit-cell parameters of the synthetic Opx crystals (Table 1) agree well with the previously reported values (Turnock et al. 1973; Giuli et al. 2002; Tarantino et al. 2002). Two starting mixes were used for the reversal experiments: one with the Mg-rich Opx (X_{Fs} = 0.05; mix *a* in Table 2), and another with the relatively Fe-rich Opx (X_{Fs} = 0.45; mix *b* in Table 2).

All experimental products were analyzed optically, by BSE imaging, and by electron microprobe. XRD was not used to analyze products of the reversal experiments to avoid grinding the samples, which could obscure any possible within-grain inhomogeneity. Optical examination was found sufficient for identifying final phases in the experiments, primarily because of the distinct optical properties of the phases. Particular care was given to verifying the presence in the run products of hematite, which was readily identified by its reddish color in transmitted light. The results of optical observations were always supported by BSE images and microprobe analysis.

Analyses were made using the University of Chicago Cameca SX-50 automated electron microprobe. The details of the analytical procedure are given in Aranovich and Berman (1997). Because of the strongly contrasting silica contents in the phases of the reaction, the problem of obtaining false orthopyroxene analyses due to probing the overlapping grains of different phases (as discussed in Aranovich and Berman 1997) was not encountered in this study.

RESULTS AND DISCUSSION

Reversals of the Opx composition buffered by Hm, Mt, and Qz were obtained at 800 and 950 °C in the pressure range 10–

25 kbar (Table 2). A major difficulty in interpreting the results of experiments on solid-solution-bearing equilibria arises from compositional inhomogeneity of experiment products (e.g., Perkins et al. 1981; Aranovich and Pattison 1995; Aranovich and Berman 1997). Fortunately, in Al-free systems this problem is not as severe as in Al-bearing ones (Perkins and Vielzeuf 1992; von Seckendorf and O'Neill 1993). In the present study, product orthopyroxene also varied in composition both within individual grains and from grain to grain. The extent of both types of heterogeneity varied depending on which half-reaction of Reaction 1 operated during a run. In the runs started with mix *a*, large overgrowths of the newly formed more Fe-rich composition were commonly observed (Fig. 1c), and many smaller grains with no clear zoning had the same composition as the outer parts of the zoned ones, and no individual Opx grains with the starting Fs content could be detected in the products of 7–10 days long runs. Runs with the relatively Fe-rich starting Opx (mix *b*) produced very narrow outer zones of the newly formed more Mg-rich composition (Fig. 1d), and numerous grains preserved starting X_{Fs} , so that it was necessary to increase the duration of the 800 °C runs with starting mix *b* to over two weeks to obtain sufficient reaction yield (Table 2). This asymmetry in the rates of forward and backward reactions appears to be a typical feature of solid-solution reactions (e.g., Aranovich and Pattison 1995; Aranovich and Berman 1997).

Following the common practice of experimental phase-equilibrium studies involving solid solution(s) (e.g., Perkins et al. 1981; Aranovich and Kosyakova 1987; Lee and Ganguly 1988; Aranovich and Berman 1997), the composition of the run product Opx most different from the starting one was accepted as the “equilibrium” composition in each particular run (Table 2). About 40 individual grains or outer parts of the zoned crystals were analyzed in search for these “most advanced” compositions in each run, and the search continued until no less than 6 individual analyses showed the same composition. For all runs, the spread of these 6–8 analyses was within the uncertainties of the microprobe method. In spite of the difficulties due to incomplete equilibration of the run products, at each given *P-T*, the most advanced compositions of Opx from complementary half-brackets converged very closely to a unique value (Fig. 2

TABLE 1. Chemical analyses and unit-cell parameters of the synthetic orthopyroxenes

Nominal 100 Fe/(Fe + Mg)	Fs5	Fs45	Fs20	Fs20†	Fs20†
Synthesis conditions*	850/10/3 unbuffered	800/15/4 unbuffered	800/15/3 unbuffered	800/15/5 HM buffer	950/20/5 HM buffer
No. of analyses	20	26	18	23	17
FeO#	3.22	27.88	13.30	12.92	13.59
MgO	36.53	18.96	28.97	30.04	29.45
SiO ₂	58.75	52.24	56.26	55.56	56.30
Total	98.50	99.08	98.53	98.52	99.34
Fe (O = 3)	0.046	0.448	0.193	0.194	0.203
Mg	0.936	0.543	0.779	0.806	0.785
Si	1.009	1.004	1.014	1.011	1.006
Unit-cell parameters (Å)					
<i>a</i> ₀	18.236	18.314	18.259	18.264	18.256
<i>b</i> ₀	8.827	8.920	8.863	8.851	8.860
<i>c</i> ₀	5.182	5.214	5.190	5.197	5.200
<i>V</i> ₀	834.1	851.8	839.9	840.1	841.1

* *T*, °C/*P*, kbar/time, days.

† Synthetic Fs20 annealed at the HM buffer (see text for discussion).

TABLE 2. Experimental data on the reaction Opx(ss) + Hm = Mt + Qz

Run no.	Starting mix	<i>P</i> , kbar	<i>T</i> °C	Duration, h	X_{Fs} fin.	Phase(s) grown
O-16	<i>a</i>	10	800	235	0.19	Opx
O-15	<i>b</i>	10	800	341	0.20	Mt+Qz
O-17	<i>a</i>	15	800	198	0.23	Opx
O-18	<i>b</i>	15	800	306	0.24	Mt+Qz
O-5	<i>a</i>	20	800	164	0.29	Opx
O-8	<i>b</i>	20	800	318	0.30	Mt+Qz
O-7	<i>b</i>	20	800	368	0.29	Mt+Qz
O-9	<i>a</i>	25	800	213	0.34	Opx
O-12	<i>b</i>	25	800	347	0.34	Mt+Qz
O-19	<i>a</i>	15	950	167	0.21	Opx
O-20	<i>b</i>	15	950	192	0.21	Mt+Qz
O-10	<i>a</i>	20	950	168	0.25	Opx
O-11	<i>b</i>	20	950	236	0.25	Mt+Qz
O-14	<i>a</i>	25	950	190	0.29	Opx
O-13	<i>b</i>	25	950	191	0.30	Mt+Qz

Notes: Starting mix *a* contained Opx with X_{Fs} = 0.05; *b* = Opx with X_{Fs} = 0.45; X_{Fs} fin. = composition of run product. All run products contained Opx + Hm + Mt + Qz. Opx most different from the starting (see text for discussion).

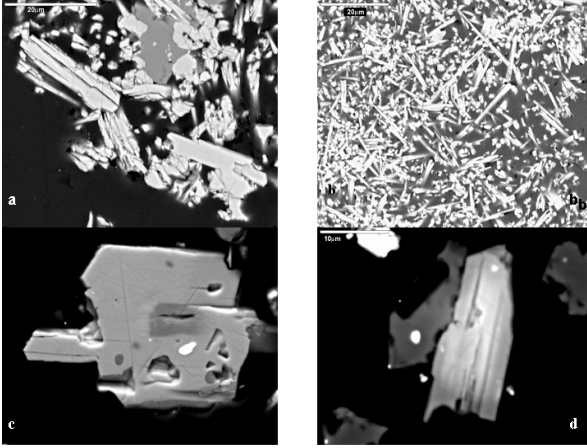


FIGURE 1. Back-scattered electron images of synthesis and reversal experiment products: (a) synthetic Opx with $X_{Fs} = 0.45$; (b) synthetic Opx with $X_{Fs} = 0.05$; note the difference in grain size between (a) and (b); (c) large more Fe-rich Opx (light grey) overgrown on the seed of starting Mg-rich composition (dark grey central part) in run O-9; (d) very thin rim of Mg-rich Opx around starting Opx with $X_{Fs} = 0.45$ in run O-12.

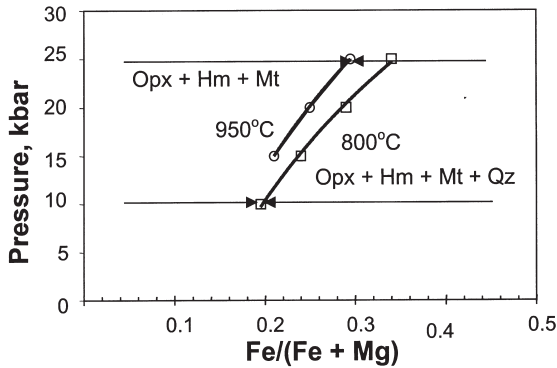


FIGURE 2. Experimental P - X_{Fe} diagram for the assemblage Opx + Hm + Mt + Qz. Results of two pairs of complementary half-brackets are shown to illustrate very good convergence of the Opx composition: arrow tails = starting Opx; arrowheads = most advanced composition of run product Opx. Curves separating three- and four-phase fields are hand-drawn through the mid-points of the brackets at 800 (squares) and 950 °C (circles).

and Table 2), which is believed to represent the equilibrium Fs content. No overlapping of the most advanced compositions of Opx in the complementary runs was observed (Fig. 2).

An important consideration of the experiments under highly oxidizing conditions is the amount of Fe^{3+} that could have entered the Opx. Although there is an indication that Fe^{3+} is negligible in the Al-free Opx (Annersten and Seifert 1981), a few additional experiments were carried out to address this problem. A synthetic Opx with $X_{Fs} = 0.2$, just off the four-phase field (Fig. 2), was annealed for a week using the double-capsule technique at 800 °C, 15 kbar and 950 °C, 20 kbar, in presence of the HM buffer. Comparison of the unit-cell edges of the Opx before and after annealing showed no systematic changes (columns 4, 5, and 6 in Table 1), thus indicating no significant Fe^{3+} in the Opx annealed under HM buffer. Good stoichiometry of the analyzed run product

Opx, calculated on the assumption of total $Fe = Fe^{2+}$, lends extra support to the above conclusion.

Equilibrium conditions of Reaction 1 are expressed as:

$$\Delta G_{T,P}^0(1) + RT \ln \frac{a_{Mt}}{a_{Hm}} - RT \ln a_{Fs} = 0 \quad (2)$$

where $\Delta G_{T,P}^0(1)$ is the standard Gibbs free energy of the reaction at T and P , a_i is activity of component i in a corresponding phase, T is temperature in K, and R is gas constant, 8.314 J/K.

Hematite and, particularly, magnetite, may dissolve some Mg at high temperature. It can be demonstrated, however, that the second term on the left hand side of Equation 2 should be very close to zero at the experimental conditions of this study. The hydrogen fugacity, in both the outer (*outr*) and the inner (*inn*) capsules at each experimental T - P , is defined by the equilibrium conditions of the reaction:



$$RT \ln f_{H_2}(outr) = + \Delta G_{T,P}^0(3) + RT \ln a_{Mt}^2/a_{Hm}^3(outr) + RT \ln f_{H_2O}(outr) \quad (4)$$

$$RT \ln f_{H_2}(inn) = + \Delta G_{T,P}^0(3) + RT \ln a_{Mt}^2/a_{Hm}^3(inn) + RT \ln f_{H_2O}(inn) \quad (5)$$

Because the thin-walled Pt capsules are permeable to hydrogen at the temperature of the experiments, the hydrogen fugacity in both the outer and the inner capsules must be equal. Subtracting Equation 4 from Equation 5, rearranging and noting that in the outer capsule both *Mt* and *Hm* are pure phases, leads to:

$$\frac{a_{Mt}^2}{a_{Hm}^3}(inn) = \frac{f_{H_2O}(outr)}{f_{H_2O}(inn)} = \frac{1}{a_{H_2O}(inn)} \quad (6)$$

where $a_{H_2O}(inn)$ is water activity in the inner capsule, which is less than 1 due to a non-negligible SiO_2 solubility under the experimental P - T (Manning 1994). At the highest T - P of the present experiments (950 °C/25 kbar) silica solubility in water, estimated by extrapolation of the Manning (1994) data is about 4 mol/kg, what corresponds to the mole fraction of H_2O , $X_{H_2O} = 0.93$. Assuming $a_{H_2O}(inn) = X_{H_2O}$ and substituting this value into Equation 6 gives

$$\frac{a_{Mt}^2}{a_{Hm}^3}(inn) = 1.075 \quad (7)$$

$$\frac{a_{Mt}}{a_{Hm}}(inn) = 1.037 \sqrt{a_{Hm}} \oplus 1 \quad (8)$$

which reduces Equation 2 to

$$\ln a_{Fs} = \Delta G_{T,P}^0(1)/RT \quad (9)$$

$\Delta G_{T,P}^0(1)$ cannot be derived directly from experiments, because the end-member reaction 1 with pure ferrosilite lies above 80 kbar, where stable pyroxene and silica polymorphs are clino-ferrosilite and coesite, respectively. Luckily, individual thermodynamic properties of the phases involved are very well constrained, so that the required values of $\Delta G_{T,P}^0(1)$ can be calculated from the existing internally consistent data sets. The results of calculations based on two recent thermodynamic

TABLE 3. Activity of ferrosilite

T (°C)	P (kbar)	X_{Fs} (exp)	$-\Delta G^0$ (B&A)	$-\Delta G^0$ (H&P)	a_{Fs} (B&A)	a_{Fs} (H&P)
800	10	0.195	15223	15280	0.182	0.180
800	15	0.240	13323	13155	0.225	0.229
800	20	0.290	11580	11125	0.273	0.287
800	25	0.340	9931	9950	0.329	0.328
950	15	0.210	16136	16505	0.205	0.197
950	20	0.250	14272	14385	0.246	0.243
950	25	0.295	12562	12480	0.291	0.293

Notes: X_{Fs} (exp) – midpoints of the experimental brackets from Table 2. Calculated from experimental data with $\Delta G^0(1)$ according to Berman and Aranovich (1996) [ΔG^0 (B&A)] and Holland and Powell (1998) [ΔG^0 (H&P)].

data sets involving Fe-bearing minerals (Berman and Aranovich 1996; Holland and Powell 1998) show amazingly good agreement (Table 3), particularly considering the differences in methodology, equations of state, and processing techniques employed in the two studies. The discrepancy in most cases does not exceed a few tens of joules, which has but negligible effect on the resulting values of a_{Fs} [compare a_{Fs} (B&A) and a_{Fs} (H&P) in Table 3]. For all experimental points, the calculated a_{Fs} values are somewhat smaller than the corresponding X_{Fs} (see Table 3), thus indicating a small negative deviation from ideality in the binary Fe-Mg Opx solid solution within the experimental P - T - X_{Fs} range. As no excess volume of mixing has been identified by the XRD studies for this binary (e.g., Tarantino et al. 2002; Giuli et al. 2002), the obtained activity values should apply to 1 bar pressure without any correction.

The excess Gibbs free energy of ferrosilite (G_{Fs}^{ex}) can be calculated from the experimentally constrained activity values according to:

$$G_{Fs}^{ex} = RT (\ln a_{Fs} - \ln X_{Fs}) \quad (10)$$

Uncertainties in G_{Fs}^{ex} , related to the experimental uncertainties in T , P , X_{Fs} , and the calculated $\Delta G_{T,P}^0$ are estimated as ± 300 – 400 J (1σ). Plots in Figure 3 compare the G_{Fs}^{ex} values of this study with those calculated according to the regular solution model as parameterized in Berman and Aranovich (1996) (curves labeled B&A in Fig. 3) and with symmetric formalism of Holland and Powell (1996) (curves labeled H&P; note that the H&P values have been normalized to 1 cation-mole in the Opx solid solution). At the 1σ level the new constraints are consistent with the B&A calibration, although just marginally at 950 °C. Taken at face value, the results of the present study indicate somewhat more negative excess enthalpy (W^H , kJ/mol) and entropy (W^S , J/K-mol) parameters of the regular solution model than those preferred by Berman and Aranovich (1996): $W^H = -3.5$, $W^S = -2.7$. Due to the very restricted temperature range of the present study, the above values must be viewed as provisional and are derived here mostly for the purpose of comparison. Much more thorough processing, similar to that of Berman and Aranovich (1996), is required for derivation of more reliable solution parameters. At the 1σ level, the new constraints are inconsistent with the H&P estimates based mostly on the site-occupancy data.

Recently Stimpfl et al. (1999) reconsidered the Fe-Mg site-occupancy data collected by XRD methods on the heat-treated Opx and concluded, contrary to most previous studies (e.g., Yang and Ghose 1994; Kroll et al. 1994), that the intracrystal-

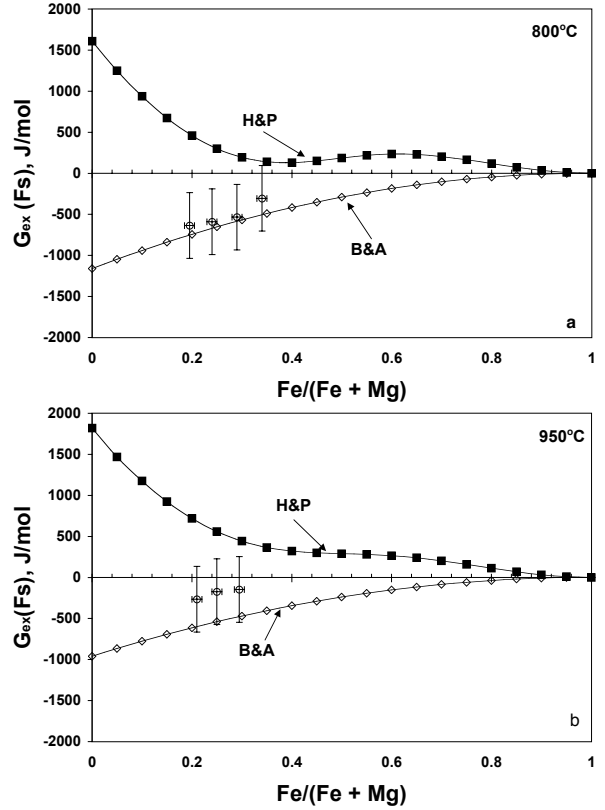


FIGURE 3. Partial excess Gibbs free energy of ferrosilite, $G^{ex}(Fs)$, in the Fe-Mg Opx solid solution after Holland and Powell (1996) (H&P), Berman and Aranovich (1996) (B&A), and new experiments (circles with uncertainty bars). Note that the H&P values have been normalized to 1 cation-mole in the Opx solid solution

line K_d values are independent of the Opx composition, at least within the range of Fs content from 19–75 mol%. This finding significantly simplified thermodynamic modeling of the site-occupancy measurements and allowed the authors to calculate the configurational entropy of mixing directly from the observed intracrystalline partitioning of Fe and Mg. The configurational entropy of mixing was then reduced to the excess entropy (S^{ex}) assuming (tacitly) electronic and vibrational contributions to be negligible. The S^{ex} values derived by Stimpfl et al. (1999) are compared in Figure 4a with the regular solution excess entropy of this study ($W^S = -2.7$ J/K-mol). As one might expect, the excess entropy calculated directly from the site occupancy data (S_{So}^{ex}) shows strong temperature dependence that is not portrayed in the phase-equilibrium-based values. The latter, nevertheless, are reasonably close to the S_{So}^{ex} values calculated for the temperature range covered by the phase-equilibrium experiments (Fig. 4a).

Implicit in the Bragg-Williams solution model is also a strong temperature dependence of the excess enthalpy (H^{ex}) (e.g., Aranovich and Kosyakova 1987; Sack and Ghiorso 1989; Holland and Powell 1996). To reconcile the S_{So}^{ex} derived by Stimpfl et al. (1999) with the G_{Fs}^{ex} constraints from the present study, as well as with the large excess heat capacity implied by equations (8.1) and (8.2) of Stimpfl et al. (1999), the strongly temperature dependent H^{ex} (dashed curves in Fig. 4b) is needed, whereas a

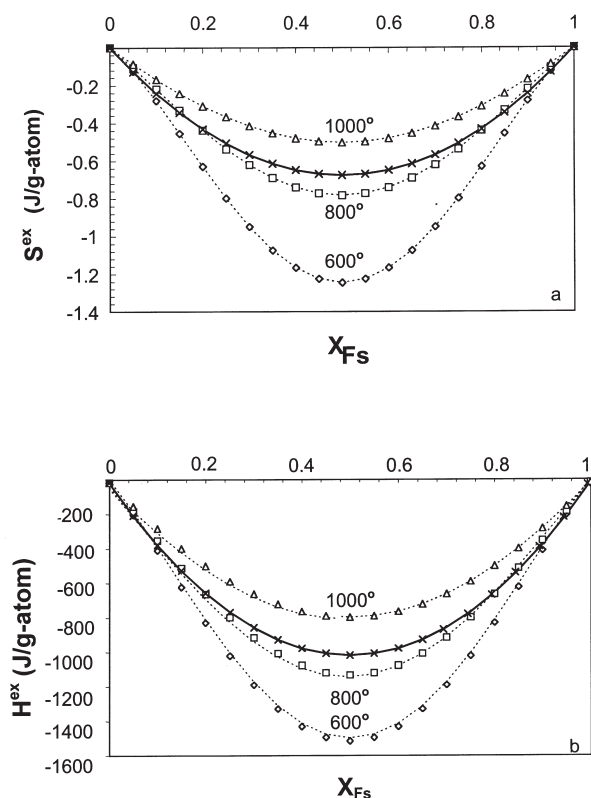


FIGURE 4. Excess entropy (a) and enthalpy (b) of the binary Fe-Mg Opx according to the site occupancy data by Stimpfl et al. (1999) (dashed curves: diamonds = 600, squares = 800, triangles = 1000 °C) and to regular solution model with the excess entropy and enthalpy parameters from the present study (bold curves marked with crosses).

regular solution model leads to a temperature-independent excess enthalpy, numerically close to the site-occupancy-based values at the temperature of the phase-equilibrium experiments (solid curve in Fig. 4b). In any event, when the site-occupancy-derived H^{ex} and S^{ex} are combined to calculate G^{ex} , the strongly temperature dependent terms related to the excess heat capacity should effectively cancel out, leading to a simple linear expression for G^{ex} as a function of temperature (e.g., Holland and Powell 1996).

O'Neill et al. (2003) have recently re-evaluated the mixing properties of the Fe-Mg olivine solid solution based on the new measurements of the activity-composition relations in magnesiowüstite. Their preferred value of the regular solution parameter for the excess Gibbs free energy of olivine at 1400 K, $W^G = 2.6$ kJ/mol (on the 1 Fe-Mg atom basis), is very close to that obtained by Berman and Aranovich (1996) for the same temperature: 2.4 kJ/mol. Applying this value to the experiments of von Seckendorff and O'Neill (1993) on the Fe-Mg partitioning between olivine and orthopyroxene results in a $W^G = 0.4$ kJ for the Opx solid solution at 1400 K, in excellent agreement with the present result ($W^G = 0.3$ kJ).

The present results support the previously drawn conclusion about a small absolute value of non-ideality of mixing in the

binary Fe-Mg Opx (e.g., Sack 1980; Aranovich and Kosyakova 1987; Lee and Ganguly 1988; Berman and Aranovich 1996; Holland and Powell 1996). It may, however, contribute significantly to the total energy of the orthopyroxene-bearing reactions whose standard Gibbs free energy is very small or in which very dilute Opx end-member is participating (as, for example, in mantle melt modeling and oxybarometry of mantle-derived ultramafic rocks).

ACKNOWLEDGMENTS

A. Koziol is thanked for donating starting mixes for the Opx synthesis, and H. O'Neill for sharing results of O'Neill et al. (2003) prior to publication. I also thank I. Steele for his generous help with the microprobe analyses, and J. Pluth and T. Dokina for assistance with the XRD measurements. This work was supported by the RFBR grant 03-05-64641.

REFERENCES CITED

- Annersten, H. and Seifert, F. (1981) Stability of the assemblage orthopyroxene-silimanite-quartz in the system MgO-FeO-Fe₂O₃-Al₂O₃-SiO₂-H₂O. *Contributions to Mineralogy and Petrology*, 77, 158–165.
- Aranovich, L.Y. and Berman, R.G. (1997) A new garnet-orthopyroxene thermometer based on reversed Al₂O₃ solubility in FeO-Al₂O₃-SiO₂ orthopyroxene. *American Mineralogist*, 82, 345–353.
- Aranovich, L.Y. and Kosyakova, N.A. (1987) The cordierite-orthopyroxene-quartz equilibrium: laboratory data on and thermodynamics of ternary Fe-Mg-Al orthopyroxene solid solutions. *Geochemistry International*, 24, 111–131.
- Aranovich, L.Y. and Newton, R.C. (1999) Experimental determination of CO₂-H₂O activity-concentration relations at 600–1000 °C and 6–14 kbar by reversed decarbonation and dehydration reactions. *American Mineralogist*, 84, 1319–1332.
- Aranovich, L.Y. and Pattison, D.R.M. (1995) Reassessment of the garnet-clinopyroxene Fe-Mg exchange thermometer: I. Reanalysis of the Pattison and Newton (1989) run products. *Contributions to Mineralogy and Petrology*, 119, 16–29.
- Berman, R.G. and Aranovich, L.Y. (1996) Optimized standard state and solution properties of minerals: I. Model calibration for olivine, orthopyroxene, cordierite, garnet, and ilmenite in the system FeO-MgO-CaO-Al₂O₃-TiO₂-SiO₂. *Contributions to Mineralogy and Petrology*, 126, 1–22.
- Bohlen, S.R., Essene, E.J., and Boettcher, A.L. (1980) Reinvestigation and application of olivine-orthopyroxene-quartz barometry. *Earth and Planetary Science Letters*, 47, 1–10.
- Fonarev, V.I. and Konilov, A.N. (1986) Experimental study of Fe-Mg distribution between biotite and orthopyroxene. *Contributions to Mineralogy and Petrology*, 93, 227–235.
- Ghiorso, M.S. and Sack, R. (1995) Chemical mass transfer in magmatic processes: IV. A revised and internally consistent thermodynamic model for interpretation and extrapolation of liquid-solid equilibria in magmatic systems at elevated temperatures and pressures. *Contributions to Mineralogy and Petrology*, 119, 197–212.
- Giuli, G., Paris, E., Wu, Z., Mottana, A., and Seifert, F. (2002) Fe and Mg local environment in the synthetic enstatite-ferrosilite join: an experimental and theoretical XANES and XRD study. *European Journal of Mineralogy*, 2002, 14, 429–436.
- Holland, T.J.B. and Powell, R. (1996) Thermodynamics of order-disorder in minerals: II. Symmetric formalism applied to solid solutions. *American Mineralogist*, 81, 1425–1437.
- Holland, T.J.B. and Powell, R. (1998) An internally consistent thermodynamic data set for phases of petrological interest. *Journal of Metamorphic Geology*, 16, 309–343.
- Kroll, H., Schlenz, H., and Philips, M.W. (1994) Thermodynamic modeling of non-convergent ordering in orthopyroxenes: a comparison of classical and Landau approaches. *Physics and Chemistry of Minerals*, 21, 555–560.
- Lee, H.Y. and Ganguly, J. (1988) Equilibrium compositions of coexisting garnet and orthopyroxene: experimental determinations in the system FeO-MgO-Al₂O₃-SiO₂, and applications. *Journal of Petrology*, 29, 93–113.
- O'Neill, H.S.C., Pownceby, M.L., and McCammon, C.A. (2003) The magnesiowüstite-iron equilibrium and its implications for the activity-composition relations of (Mg,Fe)₂SiO₄ olivine solid solutions. *Contributions to Mineralogy and Petrology*, 146, 308–325.
- Perkins, D. and Vielzeuf, D. (1992) Experimental investigation of Fe-Mg distribution between olivine and clinopyroxene: implications for mixing properties of Fe-Mg in clinopyroxene and garnet-clinopyroxene thermometry. *American Mineralogist*, 77, 774–783.
- Perkins, D., Holland, T.J.B., and Newton, R.C. (1981) The Al₂O₃ contents of enstatite in equilibrium with garnet in the system MgO-Al₂O₃-SiO₂ at 15–40 kbar and 900–1600 °C. *Contributions to Mineralogy and Petrology*, 78, 99–109.

- Sack, R.O. (1980) Some constraints on the thermodynamic mixing properties of Fe-Mg orthopyroxenes and olivine. *Contributions to Mineralogy and Petrology*, 71, 2257–2269.
- Sack, R.O. and Ghiorso, M.S. (1989) Importance of considerations of mixing properties in establishing an internally consistent thermodynamic database: thermochemistry of minerals in the system Mg_2SiO_4 - Fe_2SiO_4 - SiO_2 . *Contributions to Mineralogy and Petrology*, 102: 41–68.
- Stimpfl, M., Ganguly, J., and Molin, G. (1999) Fe^{2+} -Mg order-disorder in orthopyroxene: equilibrium fractionation between the octahedral sites and thermodynamic analysis. *Contributions to Mineralogy and Petrology*, 136, 297–309.
- Tarantino, S.C., Domeneghetti, M.C., Carpenter, M.A., Shaw, C.J.S., and Tazzoli, V. (2002) Mixing properties of the enstatite-ferrosilite solid solution: I.A macroscopic perspective. *European Journal of Mineralogy*, 14, 525–536.
- Turnock, A.C., Lindsley, D.H., and Grover, J.E. (1973) Synthesis and unit-cell parameters of Ca-Mg-Fe pyroxenes. *American Mineralogist*, 58, 50–59.
- von Seckendorff, V. and O'Neill, H.S.C. (1993) An experimental study of Fe-Mg partitioning between olivine and orthopyroxene at 1173, 1273, and 1423 K and 1.6 GPa. *Contributions to Mineralogy and Petrology*, 113, 196–207.
- Wood, B.J. and Virgo, D. (1989) Upper mantle oxidation state: Ferric iron contents of lherzolite spinels by ^{57}Fe Moessbauer spectroscopy and resultant oxygen fugacities. *Geochimica et Cosmochimica Acta*, 53, 1277–1291.
- Yang, H. and Ghose, S.H. (1994) In-situ Fe-Mg order-disorder studies and thermodynamic properties of orthopyroxenes, $(Mg,Fe)_2Si_2O_6$. *American Mineralogist*, 79, 633–643.

MANUSCRIPT RECEIVED JULY 3, 2003

MANUSCRIPT ACCEPTED OCTOBER 24, 2003

MANUSCRIPT HANDLED BY EDWARD GHENT